

A Novel Method (T-Junction with a Tilted Slat) for Controlling Breakup Volume Ratio of Droplets in Micro and Nanofluidic T-Junctions

A. Kiani Moqadam¹, A. Bedram^{2†} and M. H. Hamed¹

¹Department of Mechanical Engineering, K. N. Toosi University of Technology, Tehran, Iran

²Faculty of Imam Ali, South Khorasan Branch, Technical and Vocational University (TVU), Tabas, Iran

[†] Corresponding author, Email: a.bedram@tvu.ac.ir

(Received November 17, 2017; accepted May 4, 2018)

ABSTRACT

We propose a novel method for producing unequal sized droplets using a tilted slat in the center of a T-junctions. In the available methods for generating unequal-sized droplets such as T-junction with valve and T-junction with a heater, the minimum breakup volume ratio that is accessible is approximately 0.3 while the system of this paper can generate droplets with the volume ratio 0.05. Therefore, the manufacturing cost of the system decreases considerably because it does not need to the consecutive breakup systems for generation of small droplets. The employed method was investigated through a numerical simulation using the volume of fluid (VOF) algorithm. The simulation results are reported for micro and nano-scaled T-junctions in various tilted slat sizes, capillary numbers (a dimensionless group describes the ratio of the inertial forces to the surface tension forces) and slat angles. Our method decreases (increases) considerably the breakup time (speed of the breakup process). For example in the case $Ca=0.1$ and volume ratio 0.4, dimensionless breakup time of our method and the method of T-junction with valve are 0.25 and 3.6, respectively. The results revealed that the breakup length of the nanoscale T-junction is smaller than microscale and increases by increasing the slat angle in both scales. The results demonstrated the breakup volume ratio decreases by increasing the tilted slat length. Also the breakup volume ratio minimizes in a specific slat angle. The results showed the breakup time is reduced by decreasing the slat angle. We also found that the pressure drop of the system is almost independent of the system geometry.

Keywords: Unequal droplets; T-junction; Tilted slat; Numerical simulation; VOF; Nano; 3D.

1. INTRODUCTION

Droplet-based micro- and nanofluidic systems have found wide applications in chemical synthesis, drug delivery systems, protein crystallization, and biochemical analysis (Zhang *et al.* 2013; Zheng *et al.* 2003; Chan *et al.* 2005; Schwartz *et al.* 2004). These systems allow one to conveniently handle the amounts of fluids for various processes and better mixing of the chemical reactants inside the droplet due to flow circulation in the droplet (Tice *et al.* 2003). In recent years much research has been done on processes of these systems such as coalescence (Zhou *et al.* 2016), transport and mixing of droplets (Lee *et al.* 2016), controlling droplet size of nano emulsions (Gupta *et al.*, 2016), formation (Odera *et al.* 2014; Li X. B. *et al.* 2012; Li X. *et al.* 2016; Satoh *et al.* 2014; Bai *et al.* 2016), deformation (Wehking *et al.* 2013), breakup in symmetric and asymmetric (Du *et al.* 2015; Bedram and Moosavi 2013) geometries, and breakup behavior of a droplet in orifice microchannels (Zhu *et al.* 2016 Scientific reports journal).

By using the appropriate configuration of microfluidic

systems the proper control of the volume, generation rate, and uniformity of droplets can be obtained (Bedram *et al.* 2015 EPJE Journal; Li Y. K. *et al.* 2016). Generation of droplets with high speed and desirable sizes is prerequisite for producing chemical and pharmaceutical emulsions. Several methods have been suggested for high speed generating of equal sized droplets (Leshansky and Pismen 2009; Garstecki *et al.* 2006; Gulati *et al.* 2016; Link *et al.* 2004). These methods can only produce one specific size of droplet while biochemical and pharmaceutical industries require producing droplets with widespread range of sizes and compositions. Several techniques have been proposed for generating unequal sized droplets from an initial droplet.

One of the available methods for generation of unequal sized droplets is using a T-junction with different branches length (Link *et al.* 2004). In this method the volume ratio (the ratio of small generated droplet volume to large generated droplet volume) is approximately equal to the ratio of branches length (Link *et al.* 2004). This method controls breakup volume ratio by means of pressure drop in the

branches.

Another method is using an obstacle inside a straight channel ([Link *et al.* 2004](#)). In this method the small and large generated droplets are together after breakup process and for separating them, another process should be used.

A different method is using a λ -junction with arbitrary angles ([Deremble and Tabeling, 2006](#)). In this method the volume ratio of generated droplets is controlled by flow geometry and independent to the carrier fluid characteristics.

There is a method in which the droplets pass through a straight channel with an obstacle inside it ([Salkin *et al.* 2012](#)). In this method there is a critical value for droplet size that minimizes the critical capillary number. After breakup process, the generated drops with different sizes move together through the channel.

Another method consists of double-layer microfluidic devices with pneumatic actuator valves to control breakup of droplets ([Choi *et al.* 2010](#)). In this method the breakup process considerably depends on the shape and layout of the valve. The valve has a pressure that controls the volume ratio of generated droplets precisely and a small change in the pressure could alter volume ratio of the produced droplets. The generated droplets with various sizes are not separated by their size.

A different and new method is using an intelligent system with various valves ([Bedram *et al.* 2015 EPJE Journal](#)). This method decreases the dependence of the droplet volume ratio of the generated droplets on the inlet velocity of the system by up to 26% for long droplets.

There is a heat transfer based method in which a heater locates at one of the branches of a T-junction to control volume ratio of generated droplets ([Ting *et al.* 2006](#)). In this method for generation of low volume ratio the temperature of the fluids should increase up to 40°C that could cause some restrictions in its applications.

One of the new methods is using the vibration effects for droplets generation in microchannels ([Zhu *et al.* 2016 Microfluidics and Nanofluidics journal](#)). In this method in certain vibration frequencies, synchronized droplet generation occurs.

Another method is using different geometries in microchannels which have different angles between sub-channels ([Deremble and Tabeling, 2006](#)). In this method the breakup time decreases by reducing the angles of subchannels. But this method cannot generate the low breakup volume ratio. There are some other methods for production of unequal sized droplets such as using cross junctions ([Tan *et al.* 2008; Wu *et al.* 2008; Liu *et al.* 2011](#)). Many industries need processes that produce unequal sized droplets with low volume ratio. But a large number of the available methods does not have this ability so introduction of a new method is essential.

In this paper, we propose a novel method for production of unequal sized droplets that have some advantages

over the available methods. This method can also produce droplets with low breakup volume ratio and also increases the speed of generation of droplets significantly. For example, in a microfluidic T-junction with valve ([Bedram *et al.* 2015 EPJE journal; Bedram *et al.* 2014](#)) and a T-junction with a heater ([Ting *et al.* 2006](#)) the minimum breakup volume ratio that is accessible is about 0.48 and 0.3, respectively. In these methods for production of small droplets we should use some consecutive systems. But in the system of the present paper the accessible volume ratio of generated droplets is about 0.05 for micro and nanoscale system. In this method a tilted slat is located in the center of a T-junction. In this system generated droplets separate from each other after splitting. By manufacture of this system with an appropriate angle of titled slat, we can produce the new droplets with a specific volume ratio. The proposed system could also be used for breakup of a very short droplet even for droplets with the diameter equal to the channel width. Moreover, the breakup time in this method significantly decreases and accordingly the speed of droplets generation increases. We used a 2D numerical simulation based on the VOF algorithm in micro and nano scale systems. The results have been verified by checking grid independency and comparison of results with the benchmark problems of [Bretherton \(1961\)](#) and [Leshansky and Pismen \(2009\)](#). We study the effects of the capillary number and slat length, thickness, angle on performance parameters of the system such as breakup volume ratio, breakup length, pressure drop, and breakup time. The results of the T-junction with tilted slat also compared with a symmetric T-junction (without slat).

The presence of the gutter regions in the 3D rectangular channels causes a difference between the pressure drop results of 2D and 3D channels ([Steijn *et al.* 2010](#)). But our previous work ([Bedram *et al.* 2014](#)) indicated that in the asymmetric T-junctions with long inlet and outlet channels (as the system of the present paper), the pressure drop of the straight channels are the main pressure drop source of the system and so the effect of the gutter regions is very small. Therefore the 2D results are qualitatively very close to the 3D solution.

2. DESCRIPTION OF THE SYSTEM

The proposed system for controlling the breakup ratio of a droplet is illustrated in Fig. 1. The system uses a tilted slat as a flow controlling valve to adjust the volume ratio of generated droplets. This slat can rotate around point O . The length of the slat is l and α representing the angle between the slat and the centerline of the inlet channel. Various breakup volume ratio of the droplet can be obtained by changing geometrical properties of the slat.

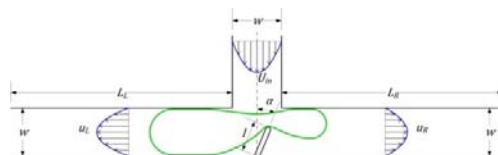


Fig. 1. Geometry of the T-junction with tilted slat and presentation of the related parameters.

If we consider w for the width of the inlet channel and branches, the dimensionless number for slat length is defined as follow.

$$\zeta = l/w \quad (1)$$

In micro (nano)-scaled system w is $20\mu m$ (100nm) and for both scales we considered $L_L = L_R = 4.5w$. The values of ζ are 0.5, 0.625, and 0.75 for microscale and a comparison is made with the nanoscale case ($\zeta = 0.5$). Also E is the entrance width of the right branch and shown in the figure with a dashed line. Initial length of the droplet in main channel is $\frac{L_d}{w} = 3$, for both nano and microscale systems.

The numerical algorithm is simulated in four different capillary numbers (0.025, 0.05, 0.075 and 0.1) for both micro and nano-channels. The capillary number (a dimensionless group describes the ratio of the inertial forces to the surface tension forces) defines as $Ca = \mu_c U_{in}/\gamma$, where μ_c represents the carrier fluid viscosity, γ is the interfacial tension between two fluids and U_{in} is the average velocity of the carrier fluid in the inlet of the system.

For nanofluidic systems the Knudsen number specifies the domination of the Navier-Stokes equations. This number defines as the following:

$$Kn = \frac{\lambda}{\ell} \quad (2)$$

Which λ is the mean free path and ℓ represents the characteristic length. Mean free path is the average distance traveled by a moving particle like a molecule between consecutive impacts. If $Kn < 10^{-2}$ the Navier-Stokes equations are valid. If $10^{-2} < Kn < 0.1$ the Navier-Stokes equations are valid but the fluid flow has slip condition on the walls. For Knudsen numbers greater than 0.1, we should use other methods such as molecular dynamics to calculate particles interactions (Crowe *et al.* 1998).

Mean free path for the fluids of the present paper (oil and water) is approximately equal to $5 \times 10^{-9} m$. We also assume the channel width as the characteristic length of the system. Therefore, $Kn = 2.5 \times 10^{-4}$ and $Kn=0.05$ for micro- and nano-scaled systems, respectively. So the Navier-Stokes equations are valid for both scales but for nanoscale system, the slip condition should be applied on the wall.

Travis *et. al.* (1997) showed the classical Navier-Stokes equations are appropriate for the fluid flow in a channel with 10 molecular diameters. Furthermore Bocquet and Charlaix (2010) fined that there is no expected deviation to the Navier-Stokes equations for the flow in the channels with the diameter larger than 1 nm. Therefore in the geometry of the present paper (with 100nm channel width) one can use the continuum hydrodynamic simulation. Also there are some researches about the simulation of the droplet breakup in the nano T-junctions that used the NS equations (Bedram *et al.* 2015 EPJE journal; Bedram *et al.* 2014).

3. NUMERICAL SIMULATION

A volume of fluid (VOF) algorithm is employed for numerical simulation. VOF is a surface tracking method for simulating the interface of non-volatile and immiscible fluids. The governing equations in VOF method are continuity and Navier-Stokes. For the incompressible, two-phase flow, these equations can be considered as the following:

$$\frac{\partial u_i}{\partial x_i} = 0, \quad (3)$$

$$\rho \left(\frac{\partial u_i}{\partial t} + u_j \frac{\partial u_i}{\partial x_j} \right) = - \frac{\partial P}{\partial x_i} + F_i + \mu \frac{\partial^2 u_i}{\partial x_j^2}, \quad (4)$$

Where u and F are the velocity vector and the continuum surface force (CSF) respectively. F is added to Navier-Stokes equation for calculating the interfacial tension. Also ρ and μ are representatives of average density and viscosity of a grid cell respectively. ρ , μ and F are calculated as follow:

$$\rho = \rho_c \phi + \rho_d (1 - \phi), \quad (5)$$

$$\mu = \mu_c \phi + \mu_d (1 - \phi), \quad (6)$$

$$F = \gamma \frac{\rho k_d \nabla \phi}{\frac{1}{2} (\rho_c + \rho_d)}, \quad (7)$$

$$k_d = \nabla \cdot \hat{n} = \nabla \cdot \frac{n}{|n|} = \nabla \cdot \frac{\phi}{|\phi|} \quad (8)$$

Where c and d are representative of continuous fluid (the major phase that carries the droplet) and dispersed fluid (droplet) respectively. ϕ is the volume fraction factor and γ is the interfacial tension and k_d is a curvature that is calculated from the divergence of the unit interface normal vector. In all of the computational cells, the volume fraction factor has a value of $0 \leq \phi \leq 1$, where $\phi = 0$ is for cells that are completely filled with dispersed phase and $\phi = 1$ is for cells which are fully filled with continuous phase. If ϕ is not equal to 0 or 1 ($0 < \phi < 1$), it means that the related cells contain both continuous and dispersed phases, which represent that the cell is in an interfacial boundary region. In order to find the exact interface location, we derive the positions with $\phi = 0.5$ in interfacial boundary regions, using a piecewise linear interface reconstruction method to construct the boundary. The volume fraction parameter is derived by the following equation:

$$\frac{\partial \phi}{\partial t} + u_i \frac{\partial \phi}{\partial x_i} = 0 \quad (9)$$

The numerical algorithm uses PISO method for pressure-velocity coupling and the momentum equation is discretized with the second-order upwind method. The convergence criterion in each time step is that the residuals be less than 0.0001. The scaled residuals calculate using the following equation:

$$R^\varphi = \frac{\sum_{P=1}^N |\sum_{nb} a_{nb} \varphi_{nb} + \psi - a_P \varphi_P|}{\sum_{P=1}^N a_P \varphi_P} \quad (10)$$

Where φ is a general variable in the cell P , N represents the number of all cells in the domain. nb denotes the neighboring cells of the cell P . a_{nb} is the coefficient of the cell P and a_{nb} is the coefficient of the neighboring cell of the cell P . ψ is a parameter that specifies the contribution of the constant part of the source term ($S = S_C + S_P \varphi$) and of the boundary conditions.

We employed a two-dimensional, transient, and multiphase model of a VOF algorithm to track the deformation and interfaces of a long droplet. The density of the continuous fluid and the droplet are 800 kg/m^3 and 1000 kg/m^3 respectively. We assume velocity constant for the inlet boundary condition and pressure constant for the outlets. Also we assume constant temperature equal to 25°C for two fluids. Therefore the energy equation isn't applicable. The viscosities for the continuous and dispersed fluids are 0.00125 Pa.s and 0.001 Pa.s respectively. The surface tension between two fluids is 0.005 N/m . The initial length for the long droplet is assumed to be $3w$.

For investigating time and grid independency, we simulated a long droplet in a symmetric T-junction in various grid sizes. The interface of the droplet at a moment that deforms in the center of junction is illustrated in Fig. 2. By comparing the result, one can obtain for grid sizes more than 19277 nodes, the change of the droplet interface is negligible. For the numerical simulations of this paper, the grid size and the time step are considered to be 26979 nodes and $8 \times 10^{-8} \text{ s}$ respectively.

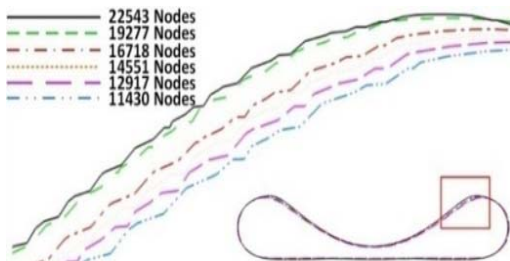


Fig. 2. Investigating grid independency of the results in a symmetric T-junction. The droplet is in the center of the symmetric T-junction. For the grids with the nodes number more than 19277 the results are grid independence. The grid size in our numerical simulations is considered to be 26979 nodes.

The numerical algorithm is validated by comparing the results to two benchmarks. Leshansky and Pismen (2009) derived an analytical relation between critical length of a droplet and capillary number as $L/w = Ca^{-0.21}$ in a symmetric T-junction (The critical length is the initial length of a droplet in a symmetric T-junction that for smaller lengths the droplet doesn't breakup). Our numerical results are compared with the Leshansky analytical relation [see Fig. 3].

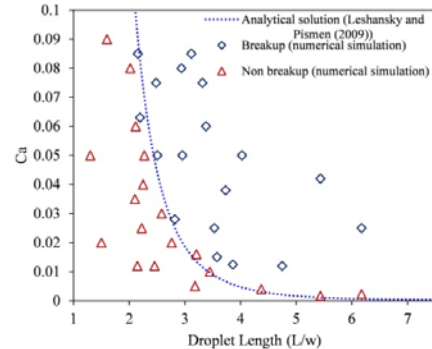


Fig. 3. Comparison of the numerical simulation results with the Leshansky and Pismen (2009) analytical relation. An excellent agreement exists.

Bretherton (1961) derive an analytical relation between velocity of a bubble with low viscosity and average velocity of fluid flow in a slender tube. He assumed that Reynolds number in the tube is small and the bubble does not contact the wall. Bretherton analytical relation is described as follow:

$$U = \bar{U} \left(1 + 1.29 \left(\frac{\mu_c U}{\gamma} \right)^{2/3} \right) \quad (11)$$

Where U is velocity of bubble and γ , μ_c , and \bar{U} are surface tension, viscosity and average velocity of carrier fluid respectively. The comparison between numerical results and Bretherton analytical relation is illustrated in Fig. 4. The numerical results of the present paper are acceptably matched with the relation of Bretherton.

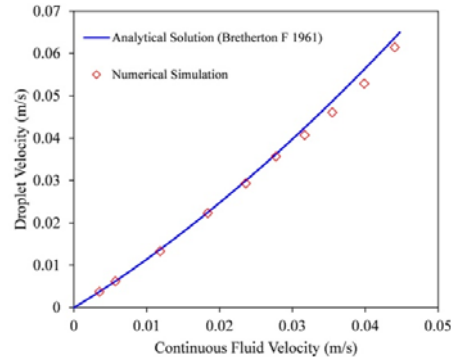


Fig. 4. Droplet velocity of a long droplet as a function of mean velocity of the carrier fluid in a tube. Comparison of the numerical simulation results with the Bretherton (1961) analytical relation shows the numerical results is acceptable.

Initial time for beginning breakup process is when the whole droplet passes through the main channel and it is considered dimensionless using the following equation:

$$t^* = \frac{(t - t_0) U_{in}}{w} \quad (12)$$

Where t^* is dimensionless breakup time. t is the time that the droplet breaks. t_0 is initial time for commencing the breakup process (Fig. 12-a). U_{in} is the velocity of the continuous fluid in the inlet and w is the channel width.

4. RESULTS AND DISCUSSION

The results of the numerical simulation of the system are presented in this section. The breakup process in a T-junction micro-channel with a tilted slat is illustrated in Fig. 5. As seen in this figure, there are two interfacial stagnation points inside of the droplet which is studied earlier by Hodges *et al.* (2004). But the difference between the streamlines of this paper with the Hodges *et al.* (2004) is due to in the Hodges paper, the droplet moves inside a long tube and in the present research, the droplet is very close to the center of a T-junction and deforms and breaks after the end of the process.

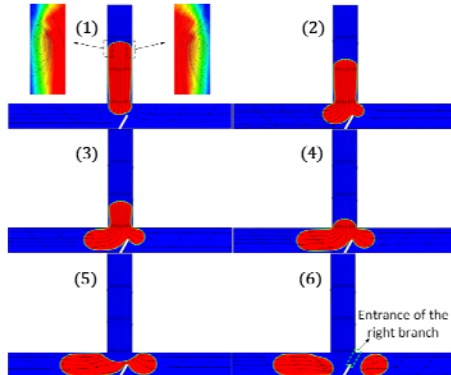


Fig. 5. Breakup process of a long droplet in a T-junction with a slat. For the shown process $Ca = 0.05$, $\zeta = 0.625$, and $\alpha = 30^\circ$.

The dimensionless time interval between stages are $\Delta t = 0.68$. Also the streamlines are shown.

The boundary condition for the process is considered constant velocity, no-slip, and constant pressure for inlet, walls, and outlets, respectively. The width of all outlets and inlet channels are equal. When the droplet reaches the slat, it deforms and goes through the two branches. The thickness of the droplet at the location of the slat becomes low until it breaks into two unequal droplets. These two generated droplets will reform fast and go toward the outlets.

The length of the branches is an important factor for a droplet breakup system. The pressure drop and the manufacturing cost of the system reduce by decreasing the length of the branches. For investigating the branch length we should define the "breakup length" parameter. The breakup length defined as the length of the droplet in the moment of breakup. Figure 6 illustrates the droplet breakup length (L), breakup length in the left channel (L_1), and the breakup length in the right channel (L_2).

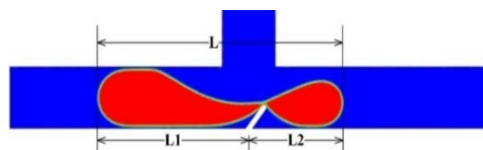


Fig. 6. Breakup length of the droplet at breakup moment. L_1 , L_2 , and L are the breakup length in the left channel, the breakup length in the right channel and the whole breakup length, respectively.

Figure 7 explains the droplet lengths as a function of the slat angle in four capillary numbers. In this figure the slat dimensionless length is $\zeta = 0.5$. The figure indicates that the droplet length increases by increasing the slat angle, because by increasing the slat angle a tunnel forms between the upper surface of the droplet and the wall (Figs. 5-5 and 6). When a droplet is deforming in the center of T-junction a distance develops between the upper interface of the droplet and the upper wall that the continuous fluid flows in it. This distance is named Tunnel. The tunnel forming extends the droplet and the droplet length increases. The droplet length in the left channel (L_1) increases linearly by increasing the slat angle. The droplet length of the left (right) channel also decreases (increases) by increasing the capillary number. It is because a smaller (larger) quantity of droplet enters the left (right) channel by increasing the capillary number. Therefore because of the constant volume of the whole droplet, the whole droplet length remains constant versus the capillary number. As seen, L_2 in the nanoscale case is less than microscale because the nanoscale case has less breakup volume ratio (Fig. 9).

As it is seen, the length of whole droplet (L) is constant versus the capillary number but increases by increasing the slat angle. In the nanoscale case ($Ca=0.075$) for $\alpha > 10$ the droplet does not break and for nanoscale case ($Ca=0.05$) only for $\alpha \leq 5$ the droplet breaks up.

One of the main advantages of the system of the present paper is producing small droplets (small breakup volume ratio) to reduce the manufacturing cost of the system. Because the available methods of generation of unequal sized droplets cannot generate small volume ratios (Bedram and Moosavi 2011; Bedram *et al.* 2015 PRE journal) and for these systems we should use two or more consecutive systems for production of droplets with small volume ratio.

The breakup volume ratio of the droplet as a function of slat angle is depicted in Fig. 9. In this figure V represents the volume of the droplet before breakup time also V_1 and V_2 denote the volume of the droplets in the right and the left channels, respectively. The breakup volume ratio is defined as:

$$\text{Breakup Volume Ratio} = V_2/V$$

As seen in Fig. 9 four capillary numbers are studied in three different ζ . As seen in the figure in the case $\zeta = 0.75$ and $Ca=0.05$, the breakup volume ratio can reach to 0.05. It is a considerable advantage for the system of the present paper respect to the available methods for generating unequal sized droplets. For example in a microfluidic T-junction with valve (Bedram *et al.* 2014; Bedram *et al.* 2015 PRE journal) and a T-junction with a heater (Ting *et al.* 2006) the minimum breakup volume ratio that is accessible is about 0.48 and 0.3, respectively. Therefore in the available methods, for production of small droplets the consecutive systems should be used and the manufacturing cost of the systems considerably increases. The curves of Fig. 9 are fitted using the second and third order polynomials.

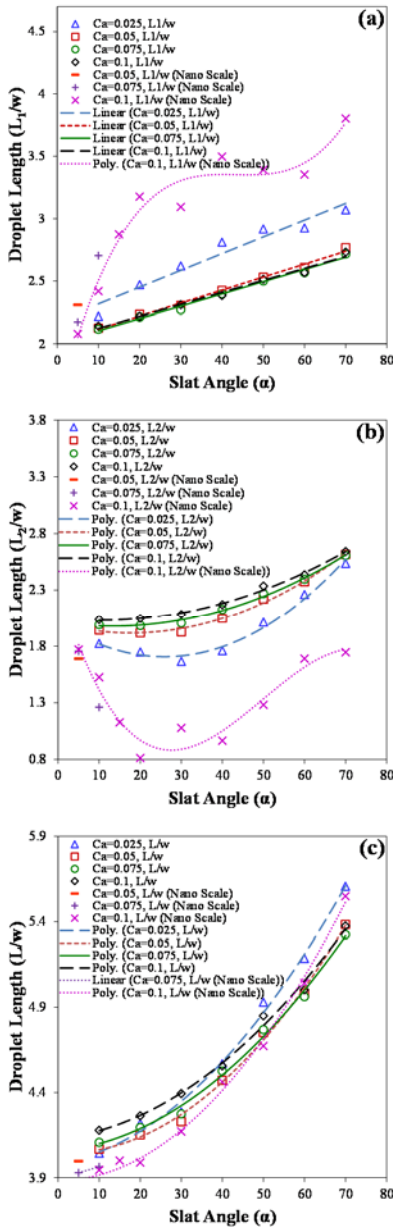


Fig. 7. Droplet length at breakup moment as a function of slat angle (α) in $\zeta = 0.5$. The droplet length became dimensionless by the channel width (w). The data is fitted with polynomial and linear trend lines.

We can change the entrance width of the right branch by modifying the slat angle. The E parameter is illustrated in Fig. 5. The width of the all of the main channels is w . According to the following relations, E becomes minimum in $\alpha \cong 26.57^\circ$.

$$\begin{aligned} E^2 &= \left(\frac{w}{2} - l \sin \alpha\right)^2 + (w - l \cos \alpha)^2 \\ \frac{\partial(E^2)}{\partial \alpha} &= 2 \left[-\frac{wl}{2} \cos \alpha + wl \sin \alpha \right] \\ \frac{\partial(E^2)}{\partial \alpha} &= 0 \rightarrow \alpha \cong 26.57^\circ \end{aligned} \quad (13)$$

The hydrodynamic resistance of the right branch maximizes by minimization of E . Therefore the flow rate of the right branch minimizes in $\alpha \cong$

26.57° . On the other hand the breakup volume ratio is approximately equal to the ratio of the flow rate of the branches (Link et al. 2004). So the volume ratio of generated droplets minimizes in $\alpha \cong 26.57^\circ$. For this reason, we can see in the Fig. 8 that the volume ratio of the generated droplets minimizes in $\alpha = 30^\circ$. Figure 8 shows the effect of E on fluid flow streamlines and subsequently breakup volume ration in various slat angles. As it can be seen in Fig. 9(c), the system with $\alpha = 30^\circ$ is the only angle that breakup doesn't occur.

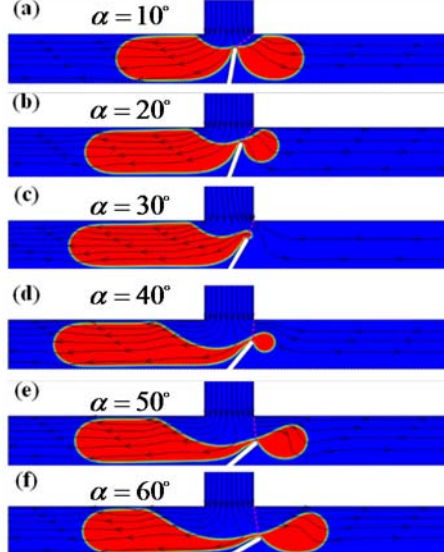


Fig. 8. Breakup volume ratio at breakup moment of systems with $\zeta = 0.75$, $Ca = 0.05$, and α between 10° to 60° . E is depicted in each picture with a purple dashed line.

As seen in the Fig. 9 the volume ratio for nanoscale cases are less than microscale cases. It is because in the nanoscale cases, when the droplet reaches to the center of T-junction, the slip condition on the walls allows the droplet to move without shear stress. So large part of the droplet flows rapidly through the left channel and subsequently pulls the remained part of the droplet to the left branch and the volume ratio decreases.

Figure 10 illustrates the breakup volume ratio as a function of the slat width. We consider three capillary numbers with $\zeta = 0.625$ and $\alpha = 20^\circ$. As seen, the breakup volume ratio decreases with the increase of the slat width. It is due to this fact that with increasing the slat width, the entrance width of the right branch (E) reduces and then the hydrodynamic resistance of the right branch increases and so the breakup volume ratio reduces. Also the results show the breakup volume ratio increases by increasing the capillary number. It is because by increasing the capillary number, the behavior of the asymmetric system becomes similar to symmetric T-junction.

Figure 11 shows the non-breakup process of a long droplet in a T-junction with a tilted slat. The streamlines of the figure show that the droplet obstructs the entrance of the right branch and the fluid flow does not enter to it.

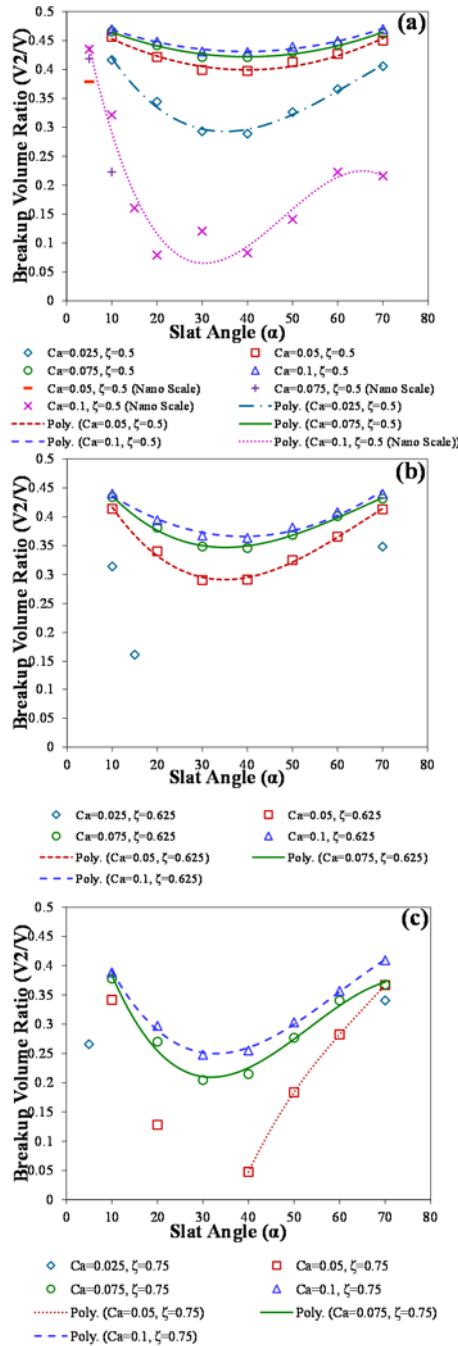


Fig. 9. Breakup volume ratio as a function of the slat angle (α). The volume ratio is calculated by dividing the smaller generated droplet (V_2) to the whole volume of initial droplet (V). The curves are fitted using second- and third-order polynomials.

The time of breakup as a function of slat angle (α) is depicted in Fig. 12. The breakup time became dimensionless using the inlet velocity and the channel width. We considered the moment that the droplet is in the state of Fig. 12-a as the initial time of the process. One of the main advantages of the method of this paper is considerably decrease (increase) in the breakup time (process speed). For example for a T-junction with valve for production of droplets with volume ratio 0.4 in $Ca=0.1$, the dimensionless breakup time is 3.6 (Bedram *et al.*

2014). But in the system of this paper in the case $Ca=0.1$ and volume ratio 0.4 the dimensionless breakup time is 0.25.

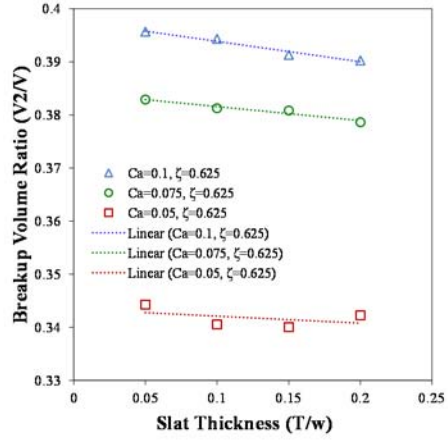


Fig. 10. Breakup volume ratio as a function of dimensionless thicknesses (T/w) of the slat. The other parameters of the system are $\zeta = 0.625$ and $\alpha = 20^\circ$. As seen, the breakup volume ratio of the generated droplets reduces linearly with increasing the slat thickness.

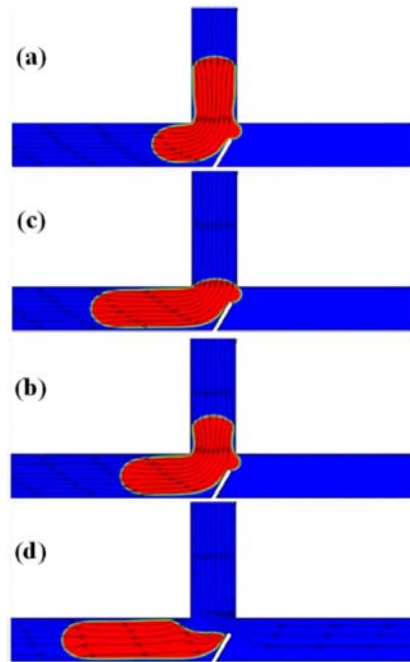


Fig. 11. Non-breakup process for the system with $\zeta = 0.75$, $Ca = 0.05$, and $\alpha = 30^\circ$. The entrance width for the right channel minimizes in about $\alpha = 30^\circ$. The cases (b) and (c) illustrate it is not any streamline in the right branch; Therefore the flow rate of the right channel is approximately equal to zero.

As seen the breakup time increases by increasing the slat angle. It is because in low slat angles when the droplet is in the center of T-junction (Fig. 5-5) the slat body reduces the droplet thickness. Therefore the droplet necking (decrease of the droplet thickness before breakup moment as seen in Fig. 5-5) happens sooner and the breakup time decreases. The results shows for microscale cases with $Ca > 0.05$ the

breakup time is independent of the capillary number. In the nanoscale cases the droplet does not break in low capillary numbers. For the case $\zeta = 0.625$ and $Ca=0.025$ the droplet does not break in $15^\circ < \alpha < 60^\circ$. Therefore because of the continuum concept, the neighboring angles (such as $\alpha = 60^\circ$ and 70°) behave similar to the non-breakup cases and have high breakup time.

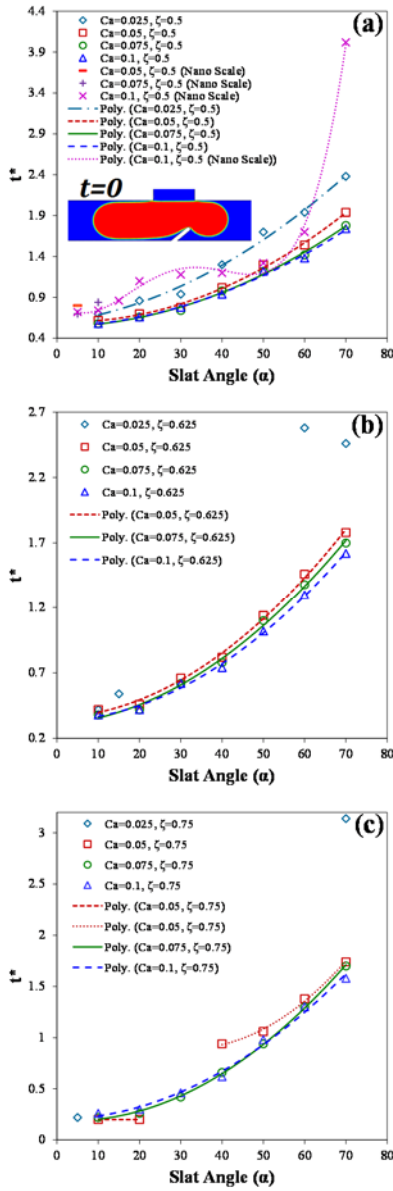


Fig. 12. Dimensionless breakup time as a function of slat angle (α). As it is shown in the figure, the initial time for measuring breakup time is when the droplet completely passes from the inlet channel. The dimensionless breakup time defines as Eq. (10).

The pressure drop of the microchannel system at the breakup moment is depicted in Fig. 13. A microfluidic T-junction has approximately maximum pressure drop at the breakup time. The system pressure drop is approximately independent of the slat angle. Also the pressure drop decreases by increasing the capillary

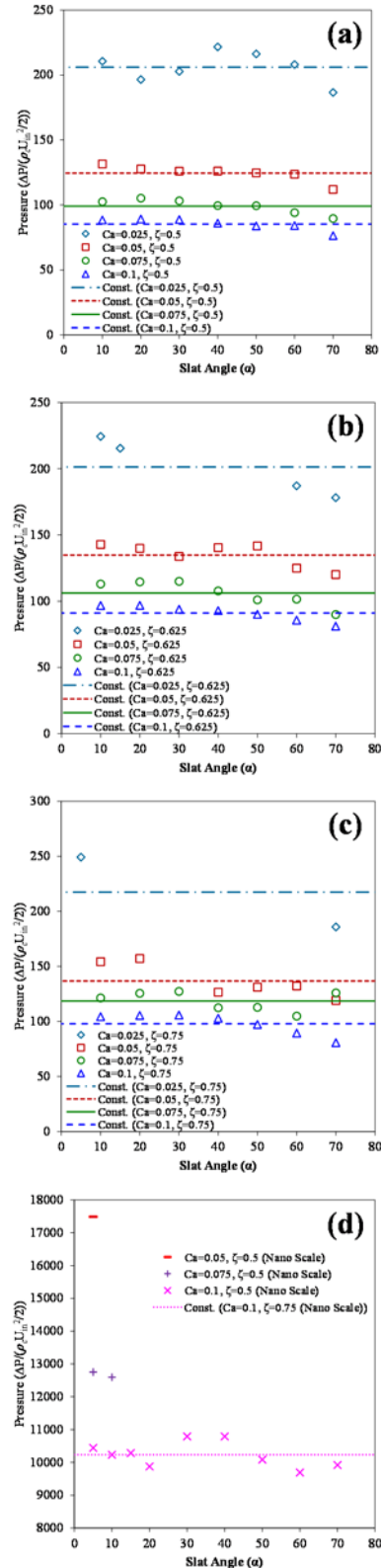


Fig. 13. Pressure drop at the breakup moment as a function of slat angle (α). Figures (a), (b), and (c) are for micro-scaled and (d) is for nano-scaled systems. The pressure drop is considered to be the difference between the pressure of the center of T-junction and the outlets of the branches. The pressure became dimensionless by dividing of the pressure to $\rho_c U_{in}^2/2$ term.

number. It is because the denominator of the y-axis parameter ($\Delta P/(0.5\rho_c U_{in}^2)$) of the Fig. 13 has the inertial term. Also the results illustrate that the pressure drop increases by increasing the slat length (ζ). It is due to the fact that by increasing the slat length the entrance width of the right branch (Fig. 5) decreases and then the pressure drop of the system increases. The pressure drop in the nanoscale cases is considerably larger than microscales cases, because in nanoscale cases the characteristic length of the system is very small.

Figure 14 depicts the pressure contour during the droplet breakup process in a micro-scaled system. It shows that pressure distribution inside a droplet is almost constant. It is due to the surface tension between the droplet and the carrier fluid. As seen, the pressure drop of fluid in the straight tube of the branches after droplet tip is negligible in comparison with the pressure difference before and after the droplet. The surface makes the droplet like a closed medium which its pressure is affected by the surrounding pressure and the surface tension. Also the droplet does not contact with the wall because a thin film of the carrier fluid exists between the droplet surface and the wall. This effect has an important application in pharmaceutical and chemical industries that the droplet composition is required to be constant. As seen in Fig. 14, the small generated droplets have relatively higher pressure comparing to larger generated droplets. It is because the difference of the pressure of inside and outside of a droplet is equal to σ/r where r is the curvature radius of the droplet interface. Therefore, the small generated droplets are higher inside pressure due to less curvature radius.

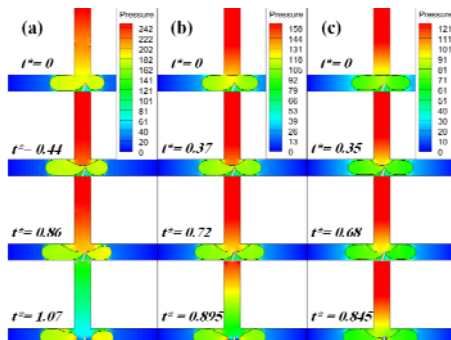


Fig. 14. Dimensionless pressure distribution ($\Delta P/(0.5\rho_c U_{in}^2)$) of breakup process in $\zeta = 0.5$ and $\alpha = 10$ microscaled system. Column (a) is for $Ca = 0.025$, (b) for $Ca = 0.05$, and (c) for $Ca = 0.1$.

Figure 15 illustrates a comprehensive sight of the parameters of the breakup process such as the volume ratio, pressure drop, length and time of the breakup. For high production rate of small droplets, we should reduce the breakup volume ratio of the droplets. Figure 15 is helpful in this condition. For example, for minimization of the volume ratio, we should use the slat angle of 40° . Therefore the droplet length, t^* and the pressure drop become 4.7, 1.32 and 210, respectively.

We reduced the initial length of the droplet (L_d) for studying the system's behavior and finding a scheme for breakup volume ratio. Figure 16 illustrates

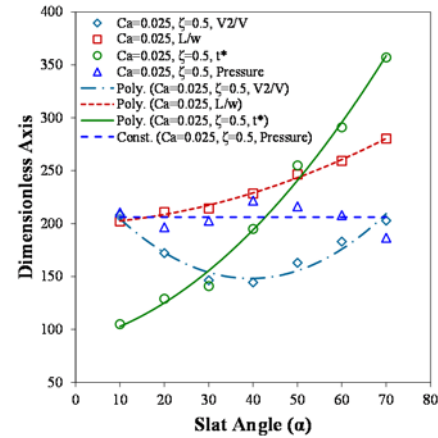


Fig. 15. Dimensionless parameters of the system with $Ca = 0.025$ and $\zeta = 0.5$. For better representation, values of volume ratio, breakup length and breakup time are multiplied by 500, 50, and 150 respectively.

a non-breakup process for the case $\frac{L_d}{w} = 1$ and a breakup process for the case $\frac{L_d}{w} = 2$. So there is a critical length in the range $1 < \frac{L_d}{w} < 2$. In the breakup moment a distance forms between the upper surface of droplet and the walls that the continuous fluid flows in it. This distance is named "tunnel". By increasing the initial length of the droplet, the tunnel width reduces (because the droplet fills the more parts of the tube). Therefore the velocity of the continuous fluid in the tunnel increases. So the hydrodynamic forces that applied on the droplet surface increases and then the droplet began to break.

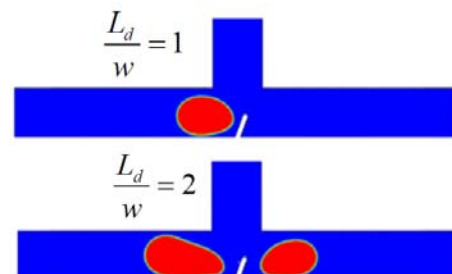


Fig. 16. Breakup process for droplets with initial length of $\frac{L_d}{w} = 1$ and $\frac{L_d}{w} = 2$. As seen, the droplet doesn't break in the case $\frac{L_d}{w} = 1$ and breaks in the case $\frac{L_d}{w} = 2$.

5. CONCLUSION

A novel method for controlling breakup volume ratio of a long droplet in micro- and nano-scaled T-junctions using tilted slat studied in this paper. The numerical simulation was based on a VOF algorithm and grid and time step independency of the systems investigated. The numerical algorithm validated by two benchmark problems and an excellent agreement was seen.

In the available methods for generating unequal-sized droplets such as T-junction with valve and T-junction with a heater, the minimum breakup volume ratio that

is accessible is approximately 0.3 while the system of this paper can generate droplets with the volume ratio 0.05. Therefore, the manufacturing cost of the system considerably decreases because it does not need the consecutive breakup systems for generation of small droplets. Our method considerably decreases (increases) the breakup time (speed of the breakup process). For example, in the case $Ca=0.1$ and volume ratio 0.4, dimensionless breakup time of our method and the method of T-junction with valve are 0.25 and 3.6, respectively. The results indicated that the droplet length increases by increasing the slat angle and the droplet length of the nanoscale case is less than microscale. The results revealed that the volume ratio of the generated droplets minimizes with minimization of the entrance of the right branch (E). Also the volume ratio of nanoscale cases is less than microscale cases.

We observed the breakup time increases by increasing the slat angle. The results showed that the system pressure drop is approximately independent of the slat angle and decreases by increasing the capillary number. The results revealed the pressure drop in the nanoscale cases is considerably larger than microscales cases. We observed the pressure distribution inside a droplet is almost constant and the droplet does not contact the wall.

REFERENCES

- Bai, L., Y. Fu, S. Zhao and Y. Cheng (2016). Droplet formation in a microfluidic T-junction involving highly viscous fluid systems. *Chemical Engineering Science* 145, 141.
- Bedram, A., A. E. Darabi, A. Moosavi and S. K. Hannani (2014). Numerical investigation of an efficient method (T-junction with valve) for producing unequal-sized droplets in micro- and nano-fluidic systems. *Journal of Fluids Engineering* 137, 031202.
- Bedram, A. and A. Moosavi (2013). Breakup of droplets in micro and nanofluidic T-junctions. *Journal of Applied Fluids Mechanics* 6(1), 81-86.
- Bedram, A. and A. Moosavi (2011). Droplet breakup in an asymmetric microfluidic T junction. *The European Physical Journal E* 34, 78.
- Bedram, A., A. Moosavi and S. K. Hannani (2015). Analytical relations for long-droplet breakup in asymmetric T junctions. *Physical Review E* 91, 053012.
- Bedram, A. A. Moosavi and S. K. Hannani (2015). A novel method for producing unequal sized droplets in micro and nanofluidic channels. *The European Physical Journal E* 38, 96.
- Bocquet, L. and E. Charlaix (2010). Nanofluidics, from bulk to interfaces. *Chemical Society Reviews* 39, 1073.
- Bretherton, F. P. (1961). The motion of long bubbles in tubes. *Journal of Fluid Mechanics* 10(2), 166-188.
- Chan, E. M., A. P. Alivisatos and R. A. Mathies (2005). High-temperature microfluidic synthesis of CdSe nanocrystals in nanoliter droplets. *Journal of the American Chemical Society* 127, 13854.
- Choi, J. H., S.-K. Lee, J.-M. Lim, S.-M. Yang and G.-R. Yi (2010). Designed pneumatic valve actuators for controlled droplet breakup and generation. *Lab on a Chip* 10, 456.
- Crowe, C. T., J. D. Schwarzkopf, M. Sommerfeld and Y. Tsuji (1998). Multiphase flows with droplets and particles. *Boca Raton (Fla.) : CRC press.*
- Deremble L. M. and P. Tabeling (2006). Droplet breakup in microfluidic junctions of arbitrary angles. *Physical Review E* 74, 035303.
- Du, W., T. Fu, C. Zhu, Y. Ma and H. Z. Li (2015). Breakup dynamics for high-viscosity droplet formation in a flow-focusing device: Symmetrical and asymmetrical ruptures. *AIChE Journal* 62(1), 325-337.
- Garstecki, P., M. J. Fuerstman, H. A. Stone and G. M. Whitesides (2006). Formation of droplets and bubbles in a microfluidic T-junction-scaling and mechanism of break-up. *Lab on a Chip* 6(3), 437-446.
- Gulati, S., K. Vijayakumar, W. W. Good, W. L. Tamayo, A. R. Patel and X. Niu (2016). Microdroplet formation in rounded flow-focusing junctions. *Microfluidics and Nanofluidics* 20(1), 2.
- Gupta, A., H. B. Eral, T. A. Hatton and P. S. Doyle (2016). Controlling and predicting droplet size of nanoemulsions: scaling relations with experimental validation. *Soft Matter* 12, 1452.
- Hodges, S. R., O. E. Jensen and J. M. Rallison (2004). The motion of a viscous drop through a cylindrical tube. *Journal of Fluid Mechanics* 501, 279-301.
- Lee, K. Y., S. Park, Y. R. Lee and S. K. Chung (2016). Magnetic droplet microfluidic system incorporated with acoustic excitation for mixing enhancement. *Sensors and Actuators A: Physical* 243, 59.
- Leshansky, A. M. and L. M. Pismen (2009). Breakup of drops in a microfluidic T junction. *Physics of Fluids* 21, 023303.
- Li, X., D. Li, X. Liu and H. Chang (2016). Ultra-monodisperse droplet formation using PMMA microchannels integrated with low-pulsation electrolysis micropumps. *Sensors and Actuators B: Chemical* 229, 466.
- Li, X. B., F.C. Li, J.C. Yang, H. Kinoshita, M. Oishi and M. Oshima (2012). Study on the mechanism of droplet formation in T-junction microchannel. *Chemical Engineering Science* 69, 340.
- Li, Y. K., K. Wang, J. H. Xu and G. S. Luo (2016). A capillary-assembled micro-device for monodispersed small bubble and droplet generation. *Chemical Engineering Journal* 293, 182-188.

- Link, D. R., S. L. Anna, D. A. Weitz and H. A. Stone (2004). Geometrically mediated breakup of drops in microfluidic devices. *Physical Review Letters* 92, 054503.
- Liu H. and Y. Zhang (2011). Droplet formation in microfluidic cross-junctions. *Physics of Fluids* 23, 082101.
- Odera, T., H. Hirama, J. Kuroda, H. Moriguchi and T. Torii (2014). Droplet formation behavior in a microfluidic device fabricated by hydrogel molding. *Microfluidics and Nanofluidics* 17, 469.
- Salkin, L., L. Courbin and P. Panizza (2012). Microfluidic breakups of confined droplets against a linear obstacle: The importance of the viscosity contrast. *Physical Review E* 86, 036317.
- Satoh, T., K. Kodama, K. Hattori, S. Ichikawa, S. Sugiura and T. Kanamori (2014). Pressure-driven microfluidic device for droplet formation with minimized dead volume. *Journal of Chemical Engineering of Japan* 47, 841.
- Schwartz, J. A., J. V. Vykoukal and P. R. C. Gascoyne (2004). Droplet-based chemistry on a programmable micro-chip. *Lab on a Chip* 4, 11.
- Steijn, V. V., C. R. Kleijn and M. T. Kreutzer (2010). Predictive model for the size of bubbles and droplets created in microfluidic T-junctions. *Lab on a Chip* 10(19), 2513-2519.
- Tan, J., J. H. Xu, S. W. Li and G. S. Luo (2008). Drop dispenser in a cross-junction microfluidic device: Scaling and mechanism of break-up. *Chemical Engineering Journal* 136(2), 306-311.
- Tice, J. D., H. Song, A. D. Lyon and R. F. Ismagilov (2003). Formation of droplets and mixing in multiphase microfluidics at low values of the reynolds and the capillary numbers. *Langmuir* 19, 9127.
- Ting, T. H., Y. F. Yap, N.-T. Nguyen, T. N. Wong, J. C. K. Chai and L. Yobas (2006). Thermally mediated breakup of drops in microchannels. *Applied Physics Letters* 89, 234101.
- Travis, K. P., B. D. Todd and D. J. Evans (1997). Departure from Navier-Stokes hydrodynamics in confined liquids. *Physical Review E* 55, 4288.
- Wehking, J. D., L. Chew and R. Kumar (2013). Droplet deformation and manipulation in an electrified microfluidic channel. *Applied Physics Letters* 103, 054101.
- Wu, L., M. Tsutahara, L. S. Kim and M. Ha (2008). Three-dimensional lattice Boltzmann simulations of droplet formation in a cross-junction microchannel. *International Journal of Multiphase Flow* 34(9), 852-864 (2008).
- Zhang, Y., H. F. Chan and K. W. Leong (2013). Advanced materials and processing for drug delivery: the past and the future. *Advanced drug delivery reviews* 65, 104.
- Zheng, B., L. S. Roach and R. F. Ismagilov (2003). Screening of protein crystallization conditions on a microfluidic chip using nanoliter-size droplets. *Journal of the American Chemical Society* 125, 11170.
- Zhou, Q., Y. Sun, S. Yi, K. Wang and G. Luo (2016). Investigation of droplet coalescence in nanoparticle suspensions by a microfluidic collision experiment. *Soft Matter* 12, 1674.
- Zhu, P., T. Kong, L. Lei, X. Tian, Z. Kang and L. Wang (2016). Droplet breakup in expansion-contraction microchannels. *Scientific Reports* 6, 21527.
- Zhu, P., X. Tang and L. Wang (2016). Droplet generation in co-flow microfluidic channels with vibration. *Microfluidics and Nanofluidics* 20, 47.